

OPTICAL DISCHARGES

DOI: 10.1070/QEL15921

Sound spectrum of a pulsating optical discharge

G.N. Grachev, A.K. Dmitriev, I.B. Miroshnichenko, A.L. Smirnov, V.N. Tishchenko

Abstract. **A spectrum of sound of an optical discharge generated by a repetitively pulsed (RP) laser radiation has been investigated. The parameters of laser radiation are determined at which the spectrum of sound may contains either many lines, or the main line at the pulse repetition rate and several weaker overtones, or a single line. The spectrum of sound produced by trains of RP radiation comprises the line (and overtones) at the repetition rate of train sequences and the line at the repetition rate of pulses in trains. A CO_2 laser with the pulse repetition rate of $f \approx 3-180$ kHz and the average power of up to 2 W was used in the experiments.**

Keywords: *pulsating optical discharge, repetitively pulsed laser radiation, shock wave, spectrum, sound.*

A pulsating optical discharge (POD) produced by a repetitively pulsed (RP) laser radiation is a source of periodic shock waves (SWs). At a high pulse repetition rate ($f \approx 100$ kHz), the mechanism of wave merging reveals: the compression phases of a SW combine and form a constant pressure component [1–3]. Repetitively pulsed radiation and the mechanism of wave merging give a chance to generate, at a large distance from the laser, the sound with the spectrum that may comprise both many lines and a single line at the laser pulse repetition rate f. A spectrum of sound produced by trains of pulses passing at a repetition rate $F \ll f$ includes the frequencies f and F, which corresponds to a simultaneous generation of ultrasound and a strong low-frequency sound, for example, infrasound. This combination of spectrum properties cannot be obtained by ordinary acoustic methods. In addition, the propagation distance of sound is limited by ultrasound absorption in air and a wide directional diagram of the low-frequency sound. For example, the intensity of an ultrasound beam with a frequency of ~50 kHz falls approximately a hundred times at a distance of ~20 m [4]. Optoacoustic experiments were performed at a low pulse repetition rate and with single pulses [5, 6].

Laboratory experiments performed with a repetitively pulsed CO_2 laser having a power of $W \approx 1-2$ kW or with two pulses of a CO_2 laser with energies of ~150 J have shown that the POD can produce sound while burning in a gas [1, 2] and on a target placed at a large distance from the laser [7–9].

The work is aimed at examining the influence of the radiation power and pulse repetition rate on a spectrum of sound generated by POD burning on a solid surface or in gas.

In the present work, laser sparks of the POD were considered as micro-explosions [6] that produce SWs. It was assumed that the pulse energy Q is well above the optical breakdown threshold. In the latter case, the parameters of SWs are approximately similar to those of a point explosion [7, 8, 10–12]. The spectrum of sound mainly depends on the frequency f and energy ηQ of laser plasma ($\eta = 0.5-0.8$). Based on experimental data we find the critical frequencies, which characterise the dependence of the spectrum on the pulse repetition rate and the power of RP radiation. The calculations utilise a shape of the SW produced under target irradiation by wide-aperture pulses of a CO_2 laser with $Q \approx 150$ J [7]. This approach makes it possible to determine the spectrum of sound produced by any source of explosive pulsed plasma. In this case, the RP radiation should satisfy the conditions of efficient SW generation by laser sparks: the density of energy q of laser beams on a target should be approximately 5–10 times greater than the optical breakdown threshold, and the pulse duration t_r should be much shorter than the time of laser spark thermal expansion. For CO_2 lasers we have $t_r \approx 1$ μs and $q \approx 10$ J cm^{-2}. The spectrum may be affected by the POD plasma torch, the material of target and ringing in the target due to the action of the SW. However, the structure of spectrum changes inessentially.

The dimensionless repetition rate of radiation pulses we may present in the form [2]

$$\omega = fR_d/c_0, \tag{1}$$

where c_0 is the velocity of sound in gas; $R_d = \sqrt[3]{b\eta Q/p_0}$ is the dynamic radius; $b \approx 1$ and $b \approx 2$ correspond to an optical breakdown in gas and on the target, respectively; and p_0 is the gas pressure. In [2, 3], the boundary frequencies ω_s and ω_0 are found such that at $\omega < \omega_s$ shock waves do not interact with each other and at $\omega > \omega_0$ the compression phases of the SW form a constant pressure component. The present work demonstrates that both the frequency ω_s and the sound spectrum depend also on a distance to the point of sound detection. In addition, there exists the frequency range $\omega > \omega_+$ wherein the main part of sound power pertains to the line with the frequency ω.

The boundary frequencies ω_s and ω_+ of the ranges are found from the following conditions:

1. At $\omega < \omega_s$, SWs do not interact with each other, the spectrum of periodic SWs comprises the main line at the fre-

G.N. Grachev, A.L. Smirnov, V.N. Tishchenko Institute of Laser Physics, Siberian Branch, Russian Academy of Sciences, prosp. Akad. Lavrent'eva 13/3, 630090 Novosibirsk, Russia; e-mail: tvn25@ngs.ru; **A.K. Dmitriev, I.B. Miroshnichenko** Novosibirsk State University, prosp. Karla Marksa, 20, 630092 Novosibirsk, Russia

Received 17 August 2015
Kvantovaya Elektronika **46** (2) 169–172 (2016)
Translated by N.A. Raspopov

quency ω and a large number of overtones (see below). The spectrum depends on the frequency ω and the duration of a single SW $t_s = 1.3R^{0.1}R_d/c_0$ [12], where $R = r/R_d$, and r is the distance from POD to the wavefront of the SW. At $R > 20$, variation of the duration t_s is small. Values of t_s well agree with data on explosions [11].

2. At $\omega_s < \omega < \omega_+$ the phases of compression interact with phases of a low pressure of SWs, and the spectrum comprises the main line at the frequency ω and several weaker overtones.

3. At $\omega > \omega_+$, compression phases of neighbouring SWs weakly interact. The duration of the compression phase of a single SW is $t_+ = 0.26R^{0.32}R_d/c_0 \approx 0.68R_d/c_0$ [7, 12], where $R \approx 20$.

4. At $\omega > \omega_0 \approx 3\omega_+$, compression phases of SWs strongly interact with each other.

By using expression (1) and the durations t_s and t_+ one can find the boundary frequencies:

$$\omega_s = f_s \frac{R_d}{c_0} = \frac{1}{t_s}\frac{R_d}{c_0} \approx 0.77R^{-0.1},$$

$$\omega_+ = f_+ \frac{R_d}{c_0} = \frac{1}{t_+}\frac{R_d}{c_0} \approx 3.8R^{-0.32} \approx 1.5.$$

In the range $\omega < \omega_s$ the spectrum of periodic SWs depends on ω and t_s. The time dependence of pressure p of a typical SW is shown in Fig. 1. The time is normalised to $t_d = R_d/c_0$. Fourier-spectra of a single SW and periodic SWs are presented in Fig. 2, where $\Omega = \nu R_d/c_0$ (ν is the spectrum frequency measured in Hz) is the dimensionless frequency. The envelope of a continuous spectrum of a single SW has a maximum at the frequency ω_s. The power-density spectrum of periodic SWs has been obtained at the SW pulse repetition rates $\omega = 0.1\omega_s = 0.07$ and $\omega = \omega_s = 0.7$. The power-density spectrum was calculated by using the fast Fourier transform. Hereinafter the spectrum is normalised to the maximum. Lines regularly fill a range under the envelope; the distance between them corresponds to the pulse repetition rate of laser pulses. At $\omega \to \omega_s$ the number of lines in the spectrum reduces. As a SW propagates, its length becomes longer, and the result is that the spectrum maximum shifts to a low-frequency range: from $\omega_s \approx 0.7$ near the POD to $\omega_s \approx 0.39$ at a distance of $R \approx 1000$.

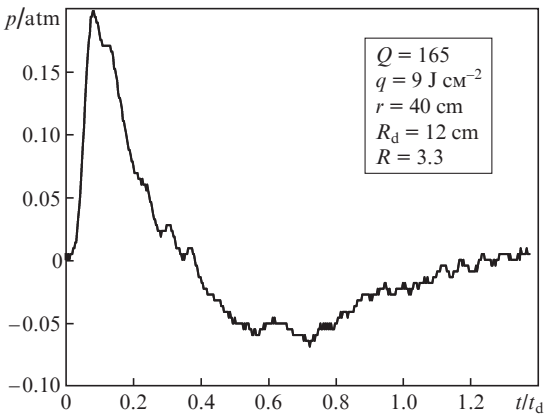

Figure 1. Pressure of a SW generated under irradiation of a steel target by laser pulses [7].

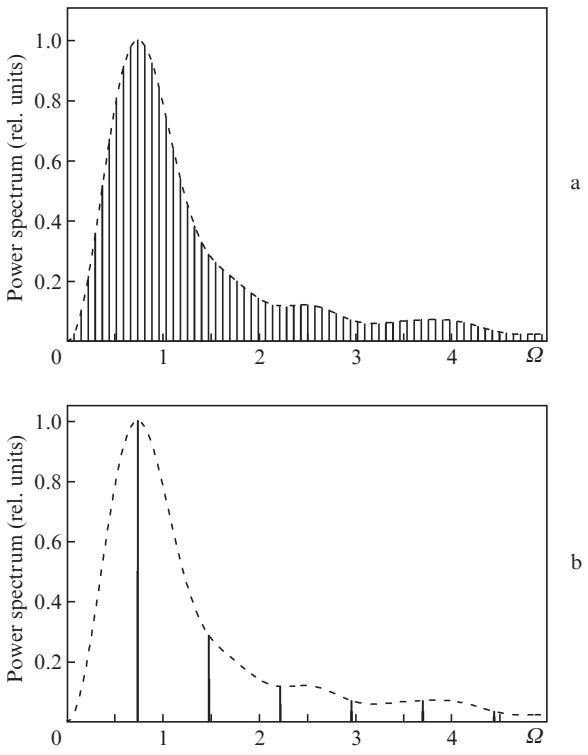

Figure 2. Calculated power-density spectra for a single ($\omega \approx 0.7$) (dashed curves) and periodic non-interacting (solid vertical curves) shock waves at ω = (a) 0.07 and (b) 0.7.

The model was verified in an experiment with a varied pulse repetition rate ($f \approx 3-180$ kHz) of a CO_2 laser [13, 14] having the average power W of up to 2 kW and the duration $t_r \approx 1$ μs. The energy of laser pulses $Q \approx 0.01-0.1$ J is not sufficient for producing a POD in air; therefore, radiation was focused onto a surface of a steel target or into an argon stream, where the optical breakdown threshold is much lower than in air. To avoid target burning, the focal spot moved along the surface. A SW pressure $p(t)$ was measured at a distance $r \approx 10-30$ cm from the POD, where $p(t)$ is much greater than the pressure of background sound (reflected sound and shock waves). The time of target irradiation and sound detection was ~30 s.

Spectra of sound generated by a POD at the laser pulse repetition rates $f = 3.4$ kHz ($\omega = 0.06$) and 15.3 kHz ($\omega = 0.29$) are shown in Fig. 3. The spectra include the main line at the frequency ω and overtones with the interval ω. The shape of the envelope is constant with increasing frequency f. Some differences between measured and calculated spectra (see Fig. 2) are explained by the fact that the sound is generated not only by the POD, but also by the target in which SWs excite oscillations. This effect has been observed in experiments with periodic trains of RP radiation. After stopping the irradiation (in a pause between trains), the sound is still detected for ~1 ms from the side of incident radiation and behind the target.

A spectrum-density power of sound in the frequency range $\omega_s < \omega < \omega_+$ is shown in Fig. 4. The POD was initiated by a RP radiation with the frequency $f = 30$ kHz ($\omega = 0.57$). The spectrum has a line at the frequency ω and overtones, the number and intensity of which reduce as ω approaches ω_+. At $f = 89$ kHz ($\omega = 1.3$) the line at the frequency ω of the laser

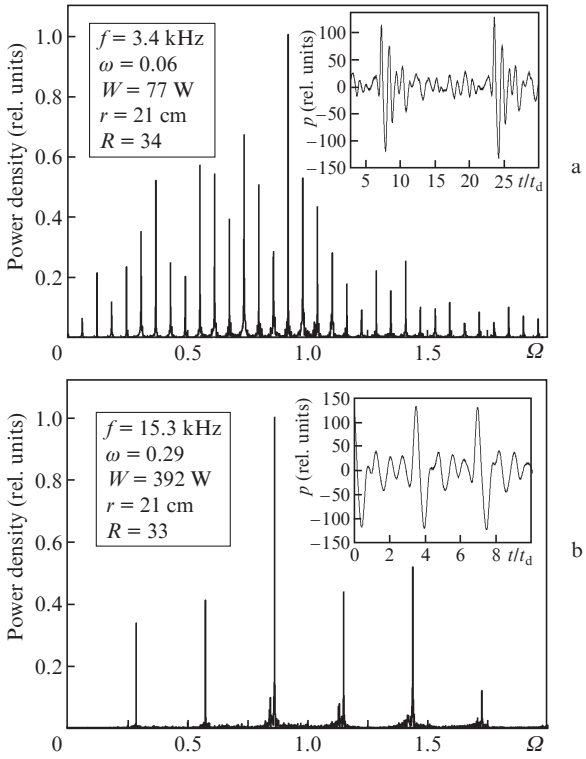

Figure 3. Power-density spectra of sound generated under target irradiation by RP laser radiation with the pulse periodic rates $f = 3.4$ (a) and 15.3 kHz (b) at $\omega_s \approx 0.55$. Sound pressure p for two periods of RP radiation (in the insets).

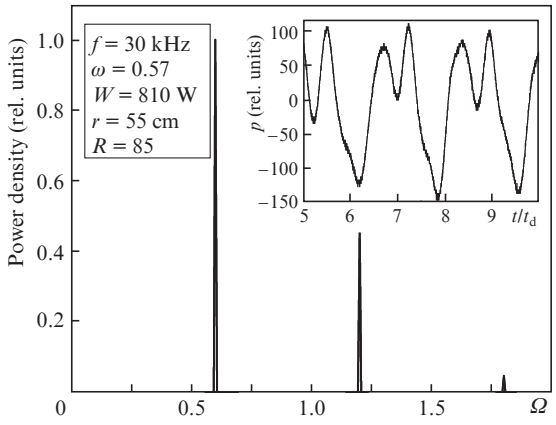

Figure 4. Power-density spectrum of sound at the repetition rate of RP radiation pulses $f = 30$ kHz and $\omega_s \approx 0.5$. Sound pressure p for two periods of RP radiation (in the inset).

pulse repetition rate prevails in the spectrum. The width $\delta\nu \approx 1$ kHz ($\delta\Omega \approx 0.015$) depends on the stability of POD burning.

In the range $\omega > \omega_+$, as ω approaches ω_0, the mechanism of wave merging becomes stronger. In this case, the POD produced by trains of RP radiation generates simultaneously ultrasound at the frequency f and a low-frequency sound at the train repetition rate F_1. In the experiment, the sound was generated at $F_1 = 0.01-6.6$ kHz ($\Omega_1 = F_1 R_d/c_0 \approx 0.000126 - 0.083$), the repetition rate of pulses in trains was $f = 153$ kHz ($\omega = 1.93$). The main line at the frequency Ω_1 and overtones at multiple frequencies comprise approximately 10% of the sound power integral over spectrum. The high-frequency part of the spectrum has a line at the frequency ω and closely located harmonics at the frequencies $\omega \pm n\Omega_1$, which are formed due to the amplitude modulation by trains with the frequency F_1.

Dependences of the boundary pulse repetition rates on the power of RP radiation, calculated by using the expression

$$f = \sqrt{\frac{(\omega c_0)^3 p_0}{2\eta W}},$$

obtained from (1) are shown in Fig. 5. At atmospheric pressure the frequency is

$$f \approx 60\sqrt{\frac{\omega^3}{2\eta W}},$$

where ηW is the average power (in kW) of RP radiation absorbed in POD; $\eta \approx 1/2$; and f is taken in kHz. The values of f_s, f_+ and f_0 correspond to $\omega = \omega_s = 0.77R^{-0.1} \approx 0.5$, $\omega_+ = 1.5$ and $\omega_0 \approx 5$. The dependence of the frequency f on the pulse energy Q has the form

$$f = \frac{\omega c_0}{\sqrt[3]{2\eta Q/p_0}}, \text{ or } f = \frac{15\omega}{\sqrt[3]{2\eta Q}}.$$

For $Q \approx 150$ J [8] we have $f_s = 1.4$ kHz, $f_+ = 4.3$ kHz and $f_0 = 14$ kHz.

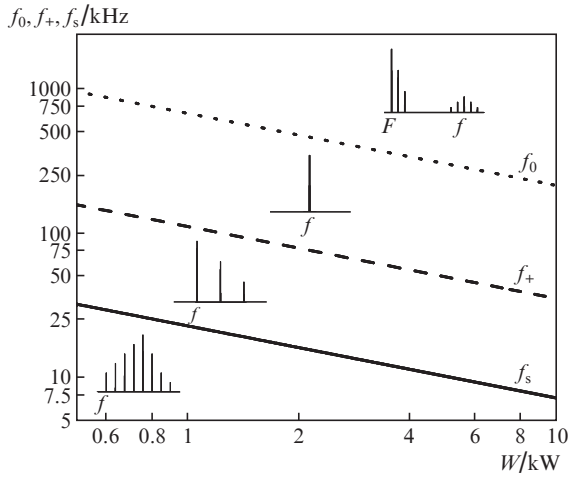

Figure 5. Boundary repetition rates of RP radiation pulses vs. the average radiation power. Typical spectra in various frequency ranges (in the insertions).

The boundary frequencies determine a transition to various spectrum structures: at $f < f_s$ the spectrum has a line at the frequency f and overtones, at $f_s < f < f_+$ it has a line at the frequency f and weak overtones, and at $f > f_+$ it has a single line. In the range $f > f_0$, the lines at the train repetition rate F and overtones prevail. Note that frequencies $f > f_0$ can be reached at a high power W and/or in the case where the POD moves at a velocity close to the velocity of sound in gas [3]. In the present work the obtained frequency is $f = 180$ kHz, whereas in [15] it was $f = 150$ kHz. A high-intensity low-frequency sound and ultrasound can be generated already at $\omega \approx 3$, $W = 10$ kW, and $f = 100$ kHz.

The model has been tested at $W < 2$ kW, $f < 180$ kHz and also under the successive irradiation of a target by two pulses [7] and with a moving POD [3].

Thus, the boundary frequencies allow one to determine a structure of the sound spectrum versus the power and the pulse repetition rate of RP laser radiation. The spectrum may comprise either a large number of lines, or the main line at the repetition rate of laser pulses and several weaker overtones, or a single line, or a single line with lateral frequencies and the lines corresponding to the repetition rate of RP radiation trains.

Acknowledgements. The work was performed in accordance with the Fundamental Research Programme of the Siberian Branch of RAS II.10.1.4 (01201374303) and was financially supported by the Ministry of Science and Education of the Russian Federation in the frameworks of the project part of the State Research Task (Project Code 1316).

References

1. Tishchenko V.N., Grachev G.N., Zapryagaev V.I., Smirnov A.V., Sobolev A.V. *Kvantovaya Elektron*., **32**, 4 (2002) [*Quantum Electron*., **32**, 4 (2002)].
2. Tishchenko V.N., Apollonov V.V., Grachev G.N., Gulidov A.I., Zapryagaev V.I., Men'shikov Ya.G., Smirnov A.L., Sobolev A.V. *Kvantovaya Elektron*., **34**, 10 (2004) [*Quantum Electron*., **34**, 10 (2004)].
3. Grachev G.N., Ponomarenko A.G., Tishchenko V.N., Smirnov A.L., Traksheev S.I., Statsenko P.A., Zimin M.I., Myakushina A.A., Zapryagaev V.I., Gulidov A.I., Boiko V.M., Pavlov A.A., Sobolev A.V. *Kvantovaya Elektron*., **36**, 5 (2006) [*Quantum Electron*., **36**, 5 (2006)].
4. Rossing Th. (Ed.) *Springer Handbook of Acoustics* (New York: Springer-Verlag, 2014).
5. Lyamshev L.M. *Usp. Fiz. Nauk*, **151**, 479 (1987) [*Sov. Phys. Usp*., **30**, 252 (1987)].
6. Prokhorov A.M., Konov V.I., Ursu I., Mikhailesku I.N. *Vzaimodeistvie lazernogo izlucheniya s metallami* (Interaction of Laser Radiation with Metals) (Moscow: Nauka, 1988).
7. Tischenko V.N., Ponomarenko A.G., Posukh V.G., Gulidov A.I., Zapryagaev V.I., Pavlov A.A., Boyarintsev E.L., Golubev M.P., Kavun I.N., Melekhov A.V., Golobokova L.S., Miroshnichenko I.B., Pavlov Al.A., Shmakov A.S. *Kvantovaya Elektron*., **41**, 10 (2011) [*Quantum Electron*., **41**, 10 (2011)].
8. Tischenko V.N., Posukh V.G., Boyarintsev E.L., Melekhov A.V., Golobokova L.S., Miroshnichenko I.B. *Opt. Atmos. Okeana*, **25** (5), 448 (2012).
9. Grachev G.N., Zemlyanov A.A., Ponomarenko A.G., Tischenko V.N., Geints Yu.E., Kabanov A.M., Pavlov A.A., Pavlov Al.A., Pogodaev V.A., Pinaev P.A., Smirnov A.L., Statsenko P.A. *Opt. Atmos. Okeana*, **26** (9), 726 (2013).
10. Yakovlev Yu.S. *Gidrodinamika vzryva* (Hydrodynamics of Explosion) (Leningrad: Sudpromgiz, 1961).
11. Smolii N.I., Tseitlin Ya.I. *Fiz. Goreniya Vzryva*, **10** (6), 919 (1974).
12. Tischenko V.N., Grachev G.N., Gulidov A.I., Zapryagaev V.I., Posukh V.G. *Proc. of the 3 Workshop on Magneto-Plasma-Aerodynamics in Aerospace Applications* (Moscow: IVTAN, 2001) pp 188–191.
13. Grachev G.N., Ponomarenko A.G., Smirnov A.L., Shulyat'ev V.B. *Proc. SPIE Int. Soc. Opt. Eng*., **4165**, 185 (2000).
14. Grachev G.N., Myakushina A.A., Smirnov A.L., Statsenko P.A. *Sb. Dokl. V Vseross. Konf. 'Vzaimodeistvie vysokokontsentrirovannykh potokov energii s materialami v perspektivnykh tekhnologiyakh i meditsine'* (V All-Russia Conference 'Interaction of Highly Concentrated Energy Fluxes with Materials in Promising Technologies and Medicine') (Novosibirsk, 2013) Vol. 1, pp 71–76.
15. Bobarykina T.A., Malov A.N., Orishich A.M., Chirkashenko V.F., Yakovlev V.I. *Kvantovaya Elektron*., **44**, 836 (2014) [*Quantum Electron*., **44**, 836 (2014)].